JGR Solid Earth

RESEARCH ARTICLE
10.1029/2021JB023723

How Does CO_2 Adsorption Alter Coal Wettability? Implications for CO_2 Geo-Sequestration

X. Sun[1,2], Y. Yao[1,2], D. Liu[1,2], and D. Elsworth[3]

[1]School of Energy Resources, China University of Geosciences, Beijing, China, [2]Beijing Key Laboratory of Unconventional Natural Gas Geological Evaluation and Development Engineering, China University of Geosciences, Beijing, China, [3]Departments of Energy and Mineral Engineering & Geosciences, Pennsylvania State University, University Park, PA, USA

Key Points:

- CO_2 adsorbs to the coal surface forcing water molecules to gather to oxygen functional group with some adsorbed water escaping from the substrate
- CO_2 adsorption converts some water-occupied sites to CO_2-occupied sites changing coal to a mixed surface comprising solid and gas pockets
- An in-situ coal wettability model clarifies mechanisms and relationships between CO_2 adsorption and coal wettability

Supporting Information:

Supporting Information may be found in the online version of this article.

Correspondence to:

Y. Yao,
yyb@cugb.edu.cn

Citation:

Sun, X., Yao, Y., Liu, D., & Elsworth, D. (2022). How does CO_2 adsorption alter coal wettability? implications for CO_2 geo-sequestration. *Journal of Geophysical Research: Solid Earth*, *127*, e2021JB023723. https://doi.org/10.1029/2021JB023723

Received 28 NOV 2021
Accepted 26 APR 2022

Author Contributions:

Conceptualization: Y. Yao
Funding acquisition: Y. Yao, D. Liu
Investigation: X. Sun
Methodology: X. Sun
Supervision: Y. Yao, D. Liu
Writing – original draft: X. Sun
Writing – review & editing: Y. Yao, D. Liu, D. Elsworth

Abstract Successful sequestration of CO_2 into coalbeds relies on sufficient capacity and rates of uptake. Storage volumes are controlled by CO_2 adsorption which in turn is affected in a complex manner by the evolving wettability of the sorption surface. However, mechanisms and interrelations between CO_2 adsorption and coal wettability remain poorly constrained – especially under recreated in situ reservoir conditions where measurements are difficult. We circumvent this difficulty by combining direct measurements of adsorbed water and inferred wettability through Nuclear Magnetic Resonance spectroscopy with mechanisms recovered from molecular dynamic (MD) simulations. The MD simulations confirm that CO_2 gas molecules adsorb to the coal pore surface, partially displace the adsorbed water, and transform the coal surface into a heterogeneous surface comprising solid interspersed with gas pockets. We then use the Cassie-Baxter equation as a basis to characterize the wettability of this heterogeneous H_2O-solid-CO_2 surface to clarify the relationship between CO_2 adsorption and coal wettability – using measurements of adsorbed H_2O, alone. This enables the first direct evaluation of coal wettability at in situ pressures of CO_2. Constrained observations suggest that water wettability weakens significantly with increasing CO_2 pressure. Under low CO_2 pressure, changes in wettability are contributed directly by CO_2 adsorption and increases in CO_2 density - when CO_2 adsorption reaches saturation at high gas pressure, then changes are determined primarily by changes in CO_2 density. We document a robust method and results for the accurate prediction of CO_2 storage capacity in coalbeds and concomitant enhanced methane recovery.

Plain Language Summary Wettability is defined as the tendency of one fluid to spread on a solid surface in the presence of other immiscible fluids. In the process of CO_2 sequestration into the coalbed, CO_2 migrates across the water-coal interface, adsorbs to the coal surface and also interacts with the water in the reservoir. The wettability highly affects CO_2 adsorption and flow, and in turn, CO_2 adsorption changes coal wettability significantly. However, how CO_2 affects wettability alteration remains unclear. Contact angle measurement is the main method for wettability evaluation, which is usually completed in an equilibrium state for coals. Thus, the effect of CO_2 adsorption is generally not considered quantitatively, limiting studies of CO_2 adsorption affecting coal wettability. Here, molecular dynamic simulation and nuclear magnetic resonance experiments were performed to investigate water-CO_2 interactions on coal surfaces. Mechanisms and relationships between CO_2 adsorption and coal wettability conclude that CO_2 adsorbs to the coal surface and converts some water-occupied sites to CO_2-occupied sites, which makes the coal surface a mixed surface comprised of solid and CO_2 gas pockets. The wettability of the mixed surface varies with the proportion of CO_2 gas pockets on the surface, which is determined by adsorption capacity.

1. Introduction

The Mauna Loa Atmospheric Baseline Observatory records a growing global atmospheric CO_2 signal reaching a peak of 420 ppm in 2021. This growing concentration may be reduced by direct capture and removal or by reducing fugitive emissions contributing to the anthropogenic signal. Related to the latter, carbon geo-sequestration (CGS) is a viable method to reduce anthropogenic CO_2 emissions (Daryasafar et al., 2019). In CGS, CO_2 is collected, purified, compressed, and then injected into storage in the subsurface. Viable storage formations comprise depleted oil and gas fields, deep saline aquifers, coal seams, salt caverns, and basalt formations (IPCC, 2005; Mosleh et al., 2019). Among these potential storage candidates, coal seams are an attractive option from two perspectives. The mode of CO_2 storage in coal reservoirs differs from in other geological hosts as it is more securely affixed by adsorption to the pore surface of the coal. The adsorption process is controlled by a

thermodynamic equilibrium between the amount of gas adsorbed and its corresponding pressure in the gas phase, that is, as long as the pressure of the fluid phase in the seam is maintained, the gas is trapped in the adsorbed state (Thakur, 2019). Thus, CO_2 can be permanently retained without an impermeable caprock surrounding and sealing the coal seams. Moreover, due to the higher affinity of CO_2 to coal with respect to methane, the injected CO_2 displaces the coalbed methane. Because of this added value, CO_2 storage in coal beds brings additional economic benefits by enhancing coalbed methane recovery (CO_2-ECBM; Mukherjee & Misra [2018]). In particular, these coal seams used for storage are usually unmineable coal as they are either too thin, too deep, too high in sulfur content and mineral matter or lack structural integrity adequate for mining economically (Folger, 2018; White et al., 2005). The available storage capacity in coal seams is estimated to be nearly 500 Gt of CO_2 with a corresponding recoverable mass of up to 50 trillion cubic meters of CH_4 (Godec et al., 2014). Since 1995, several pilot projects have been conducted in the United States, Canada, Japan, China, and Poland. These projects confirmed the provisional effectiveness and commercial viability of CO_2 storage and CO_2-ECBM subject to certain characteristics. These include successful CO_2 storage trials in the San Juan Basin, New Mexico, with some other projects deemed unsuccessful due to low CO_2 injection volume and low coalbed methane production, such as the pilot projects in the Upper Silesian Coal Basin in Poland. This emphasizes the need to understand fundamental processes controlling transport and storage in ECBM and CCS (Godec et al., 2014) – the focus of our work.

Wettability defines the affinity of one fluid to the solid surface in the presence of another immiscible fluid (Schön, 2011). Adhesive forces between the wetting fluid and the solid cause the fluid to spread across the surface and cohesive forces within the nonwetting fluid cause the fluid to retract and, through phobicity, avoid contact with the surface. Thus, the wetting phase tends to occupy the pore surface and preferentially line the small pores, with the nonwetting phase occupying the central core of the pores (Ahmed, 2010). Therefore, wettability exerts a strong control on the relative distribution of fluids within the pore space, thereby further affecting the flow of multiphase fluid in the porous medium (Arif et al., 2016b; Ibrahim & Nasr-El-Din, 2019; Plug et al., 2008). When CO_2 is injected into coal seams, it must adsorb through the available micro-and meso-pores surfaces, and thereby competes with both methane and water. Thus, the interactions between water and CO_2 necessarily redistribute the mobile water in coals, which in turn identifies the alteration in coal wettability (Gray, 1987; Sun et al., 2016). Therefore, understanding the mechanisms controlling alteration in wettability is crucial in estimating CO_2 storage efficiency in coalbeds.

Water-wetting behavior of coal changes significantly in the presence of CO_2 (Al-Yaseri et al., 2017; Arif et al., 2016b) – a feature that is also observed for pure minerals such as mica (Arif, Al-Yaseri et al., 2016), quartz (Iglauer, 2017), and feldspar (Daryasafar et al., 2019). However, unlike other minerals, coal is a strong adsorbate to CO_2, which in turn exerts a significant effect on wettability. It has been inferred that the alteration in coal wettability, from water-wet to CO_2-wet, is possibly related to CO_2 adsorption capacity (Arif, Al-Yaseri, et al., 2016; Iglauer et al., 2012). Moreover, the changes in liquid contact angle are similar to that of CO_2-adsorption on coals (Arif et al., 2016a). In addition, the wetting behavior of CO_2 on coal likely depends more on the adsorption behavior than on changes in sorbed gas density (Shojai Kaveh et al., 2012). However, how CO_2 adsorption impacts wettability and the quantitative relationship between coal wettability and CO_2-adsorption remains unclear.

The measuring of water drops or gas bubbles' contact angles is the main method to evaluate coal wettability in different CO_2 pressure environments (Al-Yaseri et al., 2017; Plug et al., 2008). Contact angle measurement of water drops on coal surfaces is strongly time-dependent, resulting from the penetration of water into the porous medium (Krainer & Ulrich, 2021; Muster & Prestidge, 2002), especially for water-wetting coals. Therefore, contact angles are typically measured as soon as possible to minimize changes in contact angle resulting from water imbibition (Arif et al., 2016a; Sarmadivaleh et al., 2015). In this case, the effect of CO_2 adsorption and CO_2-water interactions are generally ignored in contact angle measurements, intrinsically limiting studies of CO_2 adsorption affecting coal wettability to an initial state. For the measurement of CO_2 bubble contact angle, CO_2 adsorption has been considered (Sakurovs & Lavrencic, 2011; Shojai Kaveh et al., 2012) - however, CO_2 bubbles contain too little mass to allow adsorption to reach an equilibrium state. Moreover, both CO_2 adsorption and dissolution into the water must both be considered in evaluating changes in contact angle, which bring difficulties in evaluating their separate effects. In actuality, there is sufficient time (days to months) for CO_2 to migrate across the water film, adsorb to the coal surface and replace the water in subsurface reservoirs – and it is this equilibrium behavior that is therefore important in evaluating storage capacity. It is from this perspective, that we challenge

the accuracy and applicability of prior contact angle measurements to the study of in-situ wettability of coal in CO_2 environments.

We address this shortfall in the applicability of two-phase wettability measurements through highly-constrained NMR measurements of in-situ water-CO_2 interactions in coals. Molecular dynamics (MD) simulations of water-CO_2 interactions on pore surfaces are then performed to account for how CO_2 adsorption impacts the alteration of wettability. Combining the results of the MD simulations with the NMR-T_2 spectra allows the building of relationships between coal wettability and CO_2-adsorption. Thus, this study provides a novel method to evaluate the alteration in wettability under in situ conditions and thus improve the accuracy of prediction in CO_2 geo-storage capacity and related E-CBM recovery.

2. Methodology

We performed NMR measurements on coals from contrasting basins within China. The measurements of water distribution in coals define coal wettability changes in the CO_2 environment from a macro perspective. Following the macroscopic experiment results, molecular dynamic simulation was used to further study mechanisms of wettability alteration.

2.1. Samples and Experiments

Three coal samples were obtained from underground mines in the Qinshui, Ordos, and Junggar basins in China. The collected fresh coal samples were crushed and screened to particles in the size-range 0.85–2 mm in diameter using 10 and 20 mesh sieves. Subsequently, 15 g of coal particles were vacuum-dried at 60°C for 12 hr, before being saturated with distilled water for 48 hr. The remaining coal particles were used to determine maceral composition, vitrinite reflectance, and proximate analysis. After this pretreatment, the water on the particle surfaces was removed and the coals were placed into a sample cell. Different masses of gaseous CO_2 were injected into the sample cell and sorbed into the coals at 25°C. When CO_2 adsorption was complete, low field NMR-T_2 spectra of the coal samples were obtained. In addition, water contact angles on three coals were measured in air and at 25°C by using the pendent-drop method. The NMR experimental setup and details of the NMR and contact angle measurements are supplied in Text S2 of Supporting Information S1.

2.2. Theory of NMR Measurements

Details of the underlying principles of NMR measurements are discussed elsewhere (e.g., Coates et al., 1999; Howard et al., 1993). The NMR transverse relaxation time (T_2) of ^{1}H-bearing fluid is determined by bulk, surface, and diffuse relaxation, resulting in,

$$\frac{1}{T_2} = \frac{1}{T_{2B}} + \frac{1}{T_{2S}} + \frac{1}{T_{2D}} \tag{1}$$

where T_{2B} represents the bulk fluid relaxation time and is determined by the intrinsic properties of the fluid. Meanwhile, the surface relaxation time, T_{2S}, is the relaxation of ^{1}H nuclei near the surface, which is characterized by

$$\frac{1}{T_{2S}} = \rho\frac{S}{V} \tag{2}$$

where S/V is the surface-to-volume ratio of the pore and ρ is the transverse surface relaxivity. Compared to bulk relaxation, surface relaxation occurs more rapidly, therefore the surface relaxation signal appears at shorter/former relaxation times. The diffuse relaxation (T_{2D}) results from the diffusion of the hydrogen atom within different magnetic fields, which is calculated as (Coates et al., 1999)

$$\frac{1}{T_{2D}} = \frac{D(\gamma G T_E)^2}{12} \tag{3}$$

where D is the self-diffusion coefficient of water, which is 2.289×10^{-9} m^2/s at 25°C (Price et al., 1999); γ is the ^{1}H gyromagnetic ratio of a proton, as 2.68×10^8 rad/(s · T); G is field-strength gradient, which is

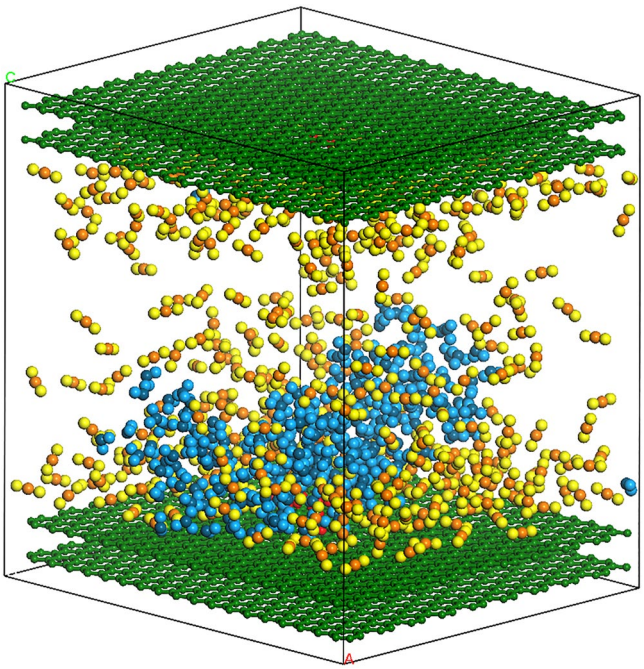

Figure 1. Three-dimensional view of the configuration of a water-CO_2- coal system at $T = 298.15$ K and $P = 6.4$ MPa. Green represents the graphene surface, orange and yellow are C and O in the CO_2, dark blue and light blue are O and H in the water and red represents hydroxy groups grafted onto the graphene surface. Note that the size of the carbon atoms (represented as green spheres) is reduced for visual clarity.

2.7×10^{-4} T/m (Yao et al., 2015); T_E is echo spacing in CPMG measurement (1.2×10^{-4} s); the calculated $\frac{1}{T_{2D}}$ is 1.438×10^{-11}/ms, which is negligible in Equation 1 (Straley et al., 1997). Therefore, Equation 1 becomes

$$\frac{1}{T_2} = \frac{1}{T_{2B}} + \frac{1}{T_{2S}} = \frac{1}{T_{2B}} + \rho\frac{S}{V} \tag{4}$$

Moreover, the T_2 signal amplitude is proportional to the number of ^{1}H nuclei, which are used to quantify the amount of water present in different occurrence states (Gubelin & Boyd, 1997).

2.3. Molecular Dynamics Simulation

Considering the complexity of the physical and chemical structures of the coal matrix, a graphene surface modified by oxygen moieties was used as a model to represent the surface of the coal. The model is built by placing two graphene sheets in parallel at a separation of 3.4 Å (You et al., 2018). Since hydroxyl is the main oxygen-containing group in coals, it was chosen as the representative oxygen-containing group to be grafted to the carbon atoms on the first graphene basal plane. The dimension of this system is $50 \times 50 \times 50$ Å^3 in the *x-, y-,* and *z*-directions respectively. Similarly, periodic boundary conditions are applied along the *x*, *y,* and *z* axes. To minimize the effect of the periodic boundary condition, the same substrate structure is placed symmetrically at the top of the control volume that contains the simulation, as shown in Figure 1. The substrate is fixed at its initial position during the simulation. For molecular interactions, the SPC/E model for water (Wu et al., 2006), and the EPM model for CO_2 are used (Harris & Yung, 1995). The details of the MD simulation are supplied in Text S3 Supporting Information S1. In the calculation, we first placed a water layer consisting of 200 molecules 10 Å above the substrate with the MD simulation conducted for water adsorption. Following this water adsorption, we place CO_2 molecules into the control volume to simulate the displacement of CO_2 to water. The MD simulations are run at different CO_2 partial pressures by varying the number of CO_2 molecules (100, 200, 400, and 800) in the repeating simulation box. The equation of the state of the gas allows the corresponding pressures (3.35, 5.30, 6.43, and 6.74 MPa) to be obtained. Moreover, to upscale the water and CO_2 distribution from the local to the whole, the box size is scaled up to $150 \times 150 \times 60$ Å^3, and 9 clusters of hydroxyl groups are evenly arranged. A total of 7,000 water molecules are first adsorbed to the surface then 10,000 CO_2 (6.43 MPa) molecules are subsequently loaded.

3. Results and Discussion

Based on NMR spectra of water in coal samples, displacement of water by CO_2 is described in the level of experiment phenomenon, and then the mechanism of CO_2-water interactions on coal surface is deciphered with MD simulations. Based on the results of the MD simulations and the NMR-T_2 spectra, the coal wettability model is built to clarify mechanisms and relationships between CO_2 adsorption and coal wettability. Besides, considering in situ reservoir condition, temperature- and pressure-dependent wettability is discussed.

3.1. Characteristics of the Coal Samples

As shown in Table 1, coal-1 is anthracite with a mean maximum vitrinite reflectance in oil ($R_{o,max}$) of 3.5% while coal-2 and coal-3 are both bituminous coals with a $R_{o,max}$ of 1.67% and 0.76%, respectively. According to vitrinite reflectance, maceral compositions, and proximate analyses, the three samples are classified as low rank and medium rank bituminous coals and high rank anthracite. As listed in Table 1, low-rank coal-3 is water-wet with a contact angle of 53°, while the medium and high-rank coals are weakly water-wet to middle-wet. The contact

Table 1
Sample Properties

NO.	Rank	$R_{o,max}$ (%)	Maceral and mineral (vol. %)				Proximate analysis (wt.%, dry)			Contact angle (°)
			V^a (%)	L^a (%)	I^a (%)	MM^a (%)	$M_{ad}{}^b$ (%)	$A_{ad}{}^b$ (%)	$C_{daf}{}^b$ (%)	
coal-1	high rank	3.5	90.7	2.8	0	6.5	1.4	16.7	88.8	89
coal-2	medium rank	1.67	77.6	19.6	0.4	2.4	0.94	12.77	85.72	78
coal-3	low rank	0.76	65.5	21.8	8.3	4.4	1.94	10.75	70.94	53

[a]*V, I, L* and *MM* represent the volume percentage of vitrinite, liptinite, inertinite, and minerals in coal composition, respectively. [b]M_{ad} and A_{ad} are the air-dry-base moisture and ash content, C_{daf} is the dry-ash-free base fixed carbon content.

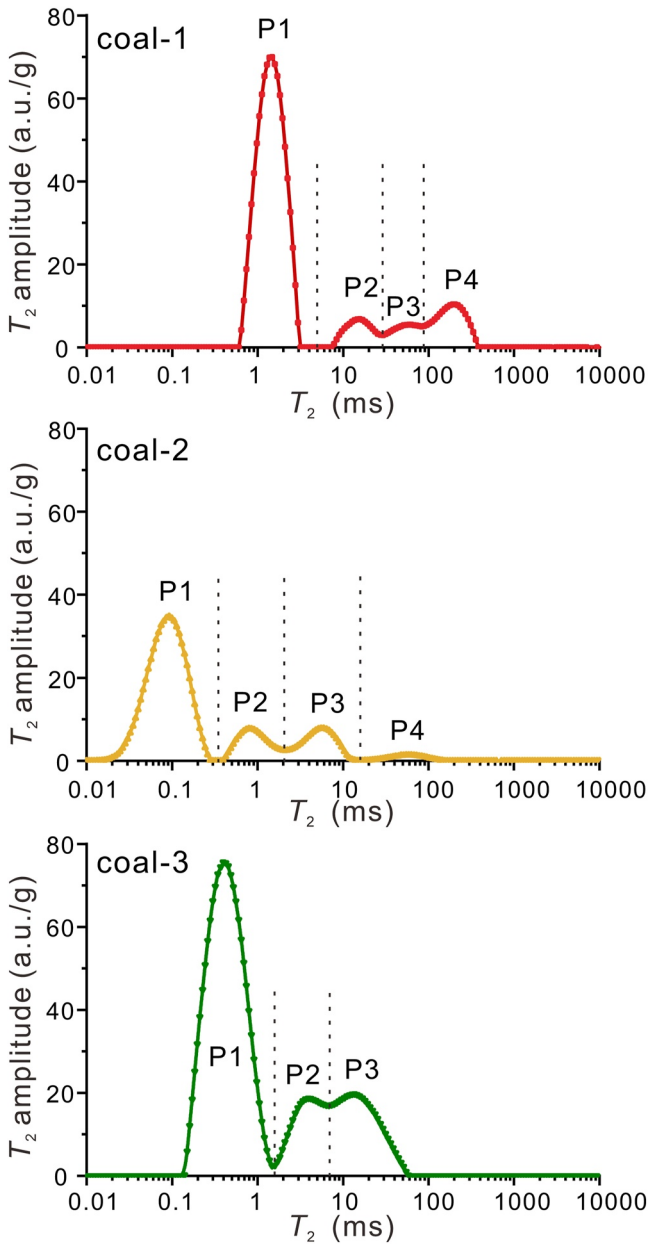

Figure 2. T_2 spectra for three water-saturated coal samples.

angles of water on the three coals vary with coal rank and maceral composition. With the coalification of coal, the number of oxygen-containing groups decreases, whereas the degree of condensation of the aromatic hydrocarbon continuously increases. Therefore, the increase of carbon content with coal rank enhances the hydrophobicity of the coal surface (Gutierrez-Rodriguez et al., 1984).

T_2 spectra of water saturated porous media provide a good proxy to determine the pore size distribution (Kleinberg et al., 1994). As shown in Figure 2, for water-saturated coal samples, there is an independent and short-time peak (P1) in the T2 spectra for all samples. According to Equation 4, the P1 peak is contributed by adsorbed water in micropores, which is dominated by surface relaxation of water (Guo & Kantzas, 2009). The P2, P3, and P4 peaks come from capillary bound water present in macropores, and the water in the pits/cavity of sample surfaces (Yao et al., 2010). For different coals, the position of the P1 peak varies, which is determined by pore size distribution and surface relaxivity. Moreover, the amplitude of P1 represents the total volume of micropores in coals, which is much larger for high rank anthracitic coal and low rank bituminous coal than that of medium rank coal. For low metamorphism coals, both micro- and mesopores are abundant. During coalification, the polycondensation of coal molecules leads to compaction and a concomitant decrease in the diameter and volume of micro- and mesopores (Nie et al., 2015). As coal rank rises continuously, the volume of micro- and mesopores increases with gas generation (Pan et al., 2015).

3.2. The Displacement of Water by CO_2

The T_2 spectra of coals were measured following CO_2 injection into the samples at controlled pressures. For all samples, the P1 peaks representing the adsorbed water decrease in amplitude as the peaks representing the bulk water or macro-capillary water increase, as shown in Figure 3. It is assumed that the CO_2 gas molecules adsorbed to the pore surface force the adsorbed water to detach from the pore surface and migrate to the center of the pores. Moreover, the capacity of CO_2 to replace the water exhibits a positive linear correlation with the Langmuir adsorption volume of CO_2 - higher adsorption capacity of CO_2 to coal yields greater replacement capacity. Besides, increasing pressure and decreasing temperature can enhance the effective displacement of water by CO_2 (Sun et al., 2016). To figure out the mechanisms by which CO_2 redistributes water, in the following discussion, we provide a molecular-scale insight into water-CO_2 interactions on coal surface.

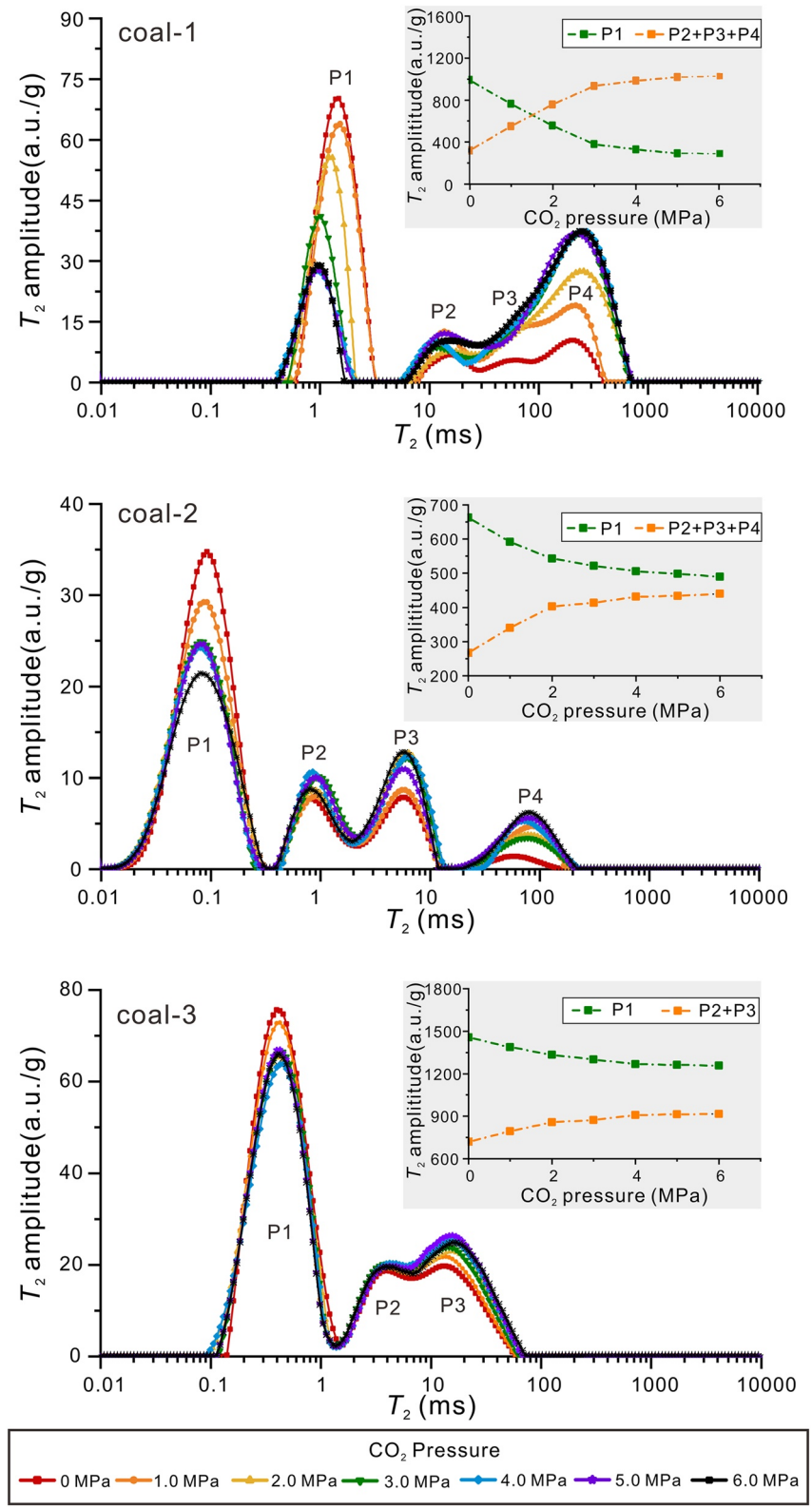

Figure 3. Change of T_2 spectra for samples after CO_2 injection at different CO_2 pressures.

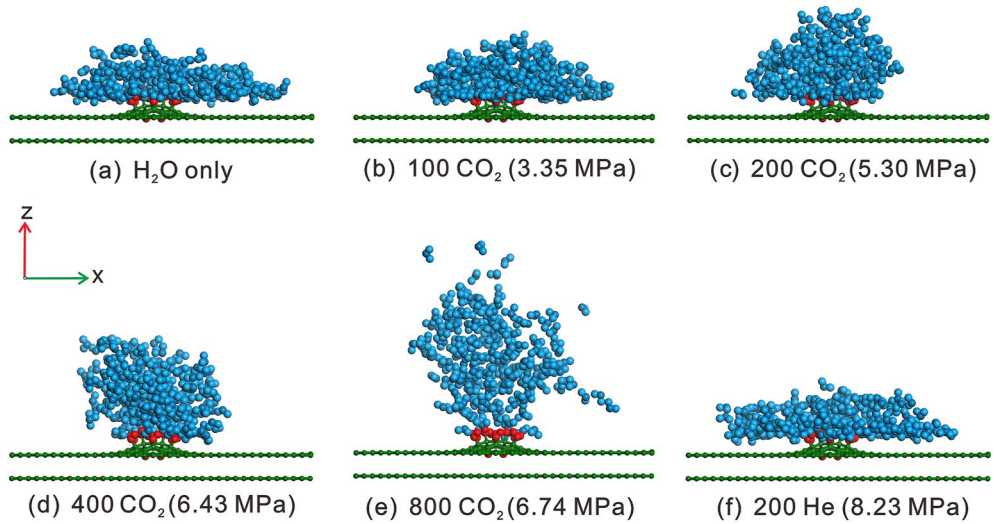

Figure 4. Distribution of water on the coal surface for different conditions. Green represents the graphene surface, dark blue and light blue are O and H in water with red represents the hydroxy groups. (The caption defining, e.g., 100 CO_2 and 3.35 MPa represent the number of added CO_2 molecules and corresponding gas pressure).

3.3. Molecular-Scale Insight Into Mechanisms of Displacement

The distribution of water on an idealized coal surface is shown in Figure 3a. Water molecules cluster around the hydroxy group with a diameter of about 15 Å. The hydroxy groups exhibit hydrophilic centers connecting H_2O molecules via strong hydrogen bonds. These attract additional H_2O molecules that gradually attach to the hydroxy groups forming a growing cluster with hydrogen bond interactions between adjacent H_2O molecules. As water clusters extend outward, the layers of water molecules become progressively smaller.

Snapshots of water molecule distributions after successively larger numbers of CO_2 molecules added (representing adsorption) are shown in Figures 4b–4e . To accurately capture changes in the water distribution, the upper graphene substrate and CO_2 molecules are set as transparent. Apparent from Figure 4 is that the H_2O molecules move gradually to the center along the *x*-direction with increasing CO_2 adsorption - the higher the CO_2 pressure the more obvious aggregation of the H_2O.

The density distribution profiles are evaluated to investigate the distribution of water molecules along the *x*-direction. The radial distribution of water molecules is shown in Figure 5 and fit to a Gaussian distribution. The standard deviation (σ) of the Gaussian distribution decreases with increasing CO_2 adsorption indicating that the width of the peak decreases with increasing gas pressure, that is, the distribution is narrower.

In addition, the density distribution profiles are obtained along the *z*-direction as a function of distance from the substrate surface (the reference point is $z = 0$), as shown in Figure 6a. Without CO_2, the density profile shows 2 distinct peaks (red line), corresponding to 2 hydration layers of water molecules. The first peak, located at 8.75 Å indicates the formation of one hydration layer of water molecules near the graphene substrate with a strong interaction force to the substrate. Thus, the concentration of water molecules is high. The second less pronounced peak, located at approximately 12.25 Å, represents the second layer of water molecules bound to the first water layer through hydrogen bonds. With continued CO_2 injection, the first peak decreases, indicating that the concentration of water molecules close to the graphene decreases, that is, those water molecules escape from surface capture and gradually migrate away from the substrate sheet.

Figure 6b also shows the radial distribution functions (RDF) of O-O between -OH and water representing the relative probability of finding any water molecule at a distance *r* from -OH groups on the graphene. As apparent in the red RDF curve of H_2O only, an elevated peak at about 2.9 Å results from the strong interaction between water molecules and -OH groups. This represents the regimented ordering of water molecules close to the surface relative to those far from the surface (Chang et al., 2015). After CO_2 adsorption, the height of the peak remains unchanged, whereas, all other peaks decrease. This suggests that the water connected to the -OH group remains

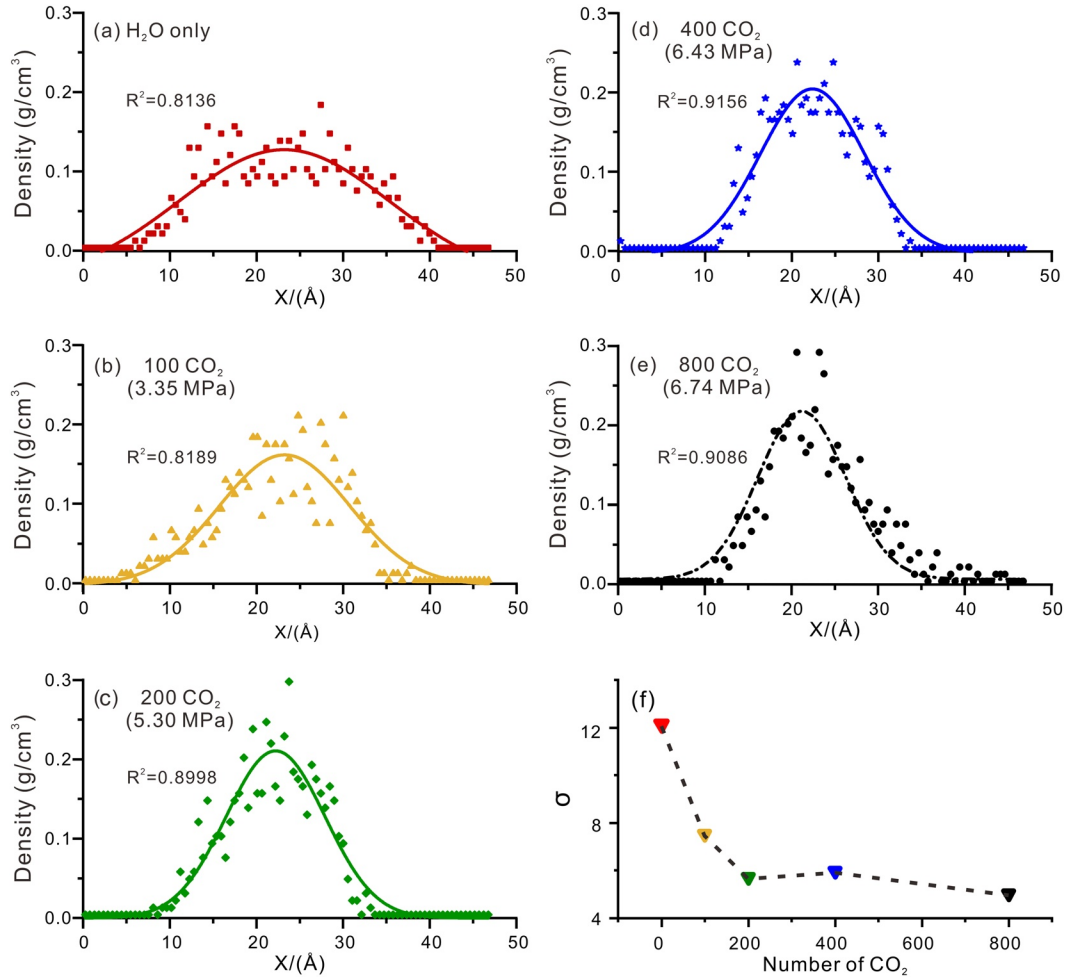

Figure 5. (a)–(e) Distribution of water molecules as a function of distance *X* and fit to a Gaussian distribution for different numbers of CO_2 molecules representing differential pressures; (f) Standard deviation (σ) of Gaussian distribution for different numbers of CO_2 molecules.

highly ordered, however, as water molecules migrate away from the substrate and the interaction force becomes weaker, its structure becomes more disordered.

In general, when CO_2 adsorption occurs on coal, water molecules gather gradually along the *x*-direction and onto the -OH group. Meanwhile, water molecules move away from the substrate in the perpendicular (z-) direction. For CO_2 molecules, the Van der Waals interaction provides a dominant contribution to their adsorption to the coal. The absolute value of the interaction energy for CO_2 on graphene is larger than that of H_2O (P. H. Huang & Chen., 2016), that is, the interactions between CO_2 and graphene are stronger than that between H_2O and graphene. Thus, CO_2 adsorbs to coal and displaces the peripheral water molecules. With increasing CO_2 pressure, water escaping from the substrate becomes more obvious. Those replaced water molecules may move to the center of the pore, as shown in Figure 3e. MD simulations provides a microscopic explanation for the CO_2 displacing H_2O.

In addition, a comparative simulation was conducted by loading 200 helium molecules into the simulation box instead of CO_2. As shown in Figure 4f, the water distribution is almost the same as that in Figure 4a. Comparing the molecular density profiles along the *z*-direction and the RDF of O-O, in each helium-only and CO_2-only condition, suggests that helium exerts nearly no influence on the distribution of water on the graphene surface.

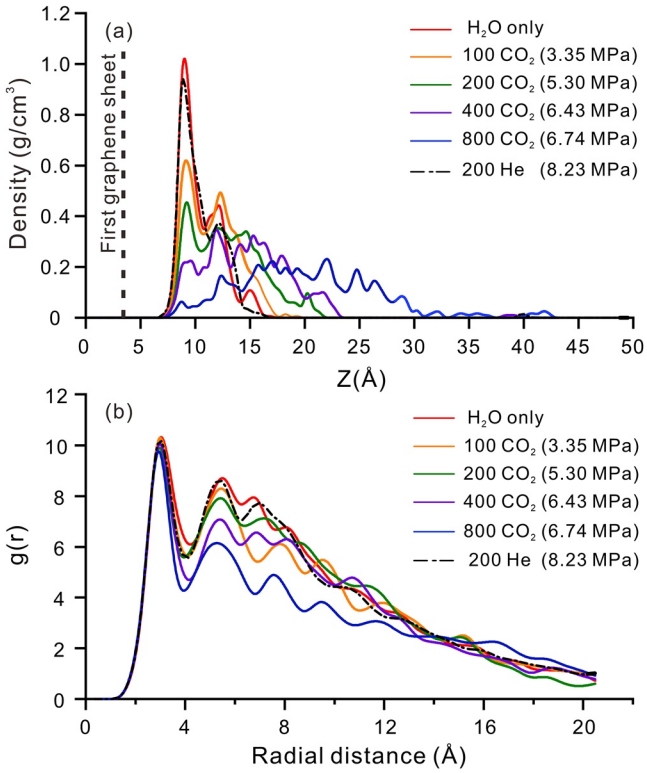

Figure 6. (a) Density profiles of water molecules along the z-direction and (b) radial distribution functions for O-O between -OH and water at different CO_2 loadings.

3.4. Mechanisms Responsible for the CO_2 Adsorption Effect on Coal Wettability

When the simulation is scaled-up, the effects of CO_2 on the distribution of water on the surfaces of coal become more obvious. As shown in Figure 7, the surface of the coal was initially covered with water. After the loading of CO_2 molecules, to represent the presence of the gas, patchy distribution of water and CO_2 then develops. These results provide microscopic verification of the change in wettability driven when CO_2 attaches itself to the coal surface, converting some water-occupied sites on the coal surface to CO_2-occupied sites. Those CO_2-occupied sites are entirely hydrophobic. As a consequence, CO_2 adsorption transforms the uniformly water-covered coal surface into a mixed surface comprised of solid coal and CO_2 gas pockets, which behave heterogeneously with respect to the water-wettability of coal.

The heterogeneous surface wettability of materials is typically predicted by,

$$\cos\theta^* = \frac{\sum_1^i f_i\,(\gamma_{i,SG} - \gamma_{i,SL})}{\gamma_{LG}} = \sum_1^i f_i \cos\theta_i \tag{5}$$

in which the θ^* is the average contact angle and γ_{LG}, γ_{SL}, γ_{SG} are the interfacial tensions at the liquid/air, solid/liquid, and solid/air (vapor) interfaces, respectively. Each material is characterized by its own surface tension coefficient $\gamma_{i,SG}$ and $\gamma_{i,SL}$, and by its decimal fraction f_i in the substrate surface, with $f_1 + f_2 + \ldots f_n = 1$. The angle θ_i is the instinct contact angle between the liquid and each pure substrate. Equation 5 is easily derived by considering free energy equilibrium (Bormashenko, 2009), also represented by the Cassie-Baxter equation (Bormashenko, 2008; Cassie & Baxter, 1944). In our MD model, the mixed surface evolves as comprised of solid and CO_2 gas pockets, with contact angles θ_1 and π, respectively. Thus, f_1 is the ratio of the solid-liquid interface to the total area and f_2 is the ratio of the area occupied by CO_2, as,

$$\cos\theta^* = f_1\cos\theta_1 - f_2 = f_1\,(1 + \cos\theta_1) - 1 \tag{6}$$

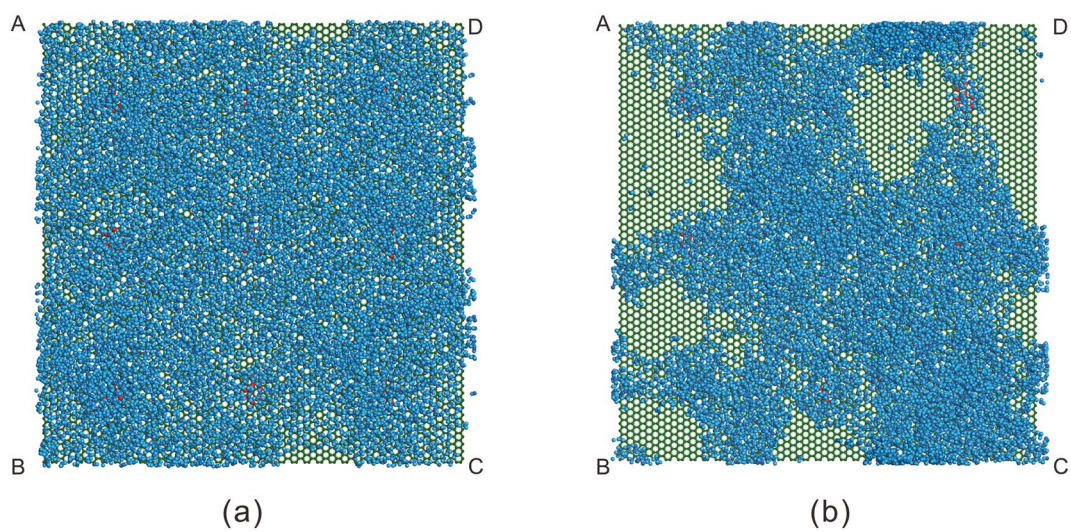

Figure 7. Water distribution both (a) before and then (b) after loading with 10,000 CO_2 molecules. Green is the graphene surface, dark blue and light blue are O and H in water and red represents hydroxy groups grafted to the graphene (CO_2 molecules are set as transparent and are therefore invisible).

Obtaining the fraction f_1 (solid-liquid interface area) then becomes the key to calculating the average contact angle θ^*, as shown in Equation 6. When water is in contact with coal on the surface, surface relaxation signals are generated in the NMR measurement. As discussed in Section 3.1, the P1 peak represents water interacting with the solid coal surface. When coal pores are completely filled with water, then the pore surface is also completely covered with water and f_1 is unity. With the injection of CO_2, water molecules are displaced by the CO_2 and f_1 decrease accordingly, that is, f_1 is the percentage of water that has not been displaced by CO_2. Thus, f_1 may be determined from the displacement capacity, which can be obtained from the P1 peak measured under different incremented CO_2 pressures. A positive linear correlation exists between the displacement capacity and the adsorption capacity of CO_2 - thus, f_1 is negatively correlated with adsorption capacity (Sun et al., 2016). The more CO_2 that adsorbs to the coal surface, the more water is displaced and therefore the smaller the fraction of the surface, f_1. Notably, displacement capacity is also related to other factors, such as clay content and porosity, thus, f_1 is also feasibly slightly influenced by those factors.

In summary, CO_2 adsorption transforms the coal surface into a mixed solid and gaseous surface, on which the contact angle may be evaluated from Equation 6. Moreover, f_1 in Equation 6 is determined by CO_2 adsorption capacity. Therefore, a clear link is established between how adsorption affects wettability and the relationship between them.

3.5. In Situ Predictions of Coal Wettability at Elevated CO_2 Pressures

Since fluid pressure varies significantly with reservoir depth, its effect on in situ wettability of the CO_2-water-coal system must be comprehensively understood. Based on the above-noted mechanisms, in-situ coal wettability is capable of being predicted under different CO_2 pressures.

The Young-Laplace equation defines the force equilibrium between the three phases in contact (water, CO_2, and pure substrate) and enables the contact angle (θ_1) to be evaluated as,

$$\cos\theta_1 = \frac{(\gamma_{SG} - \gamma_{LS})}{\gamma_{LG}} \tag{7}$$

For deionized water and a mineral surface at a constant temperature, a practical relationship was derived with the sharp-kink approximation and the Young-Laplace equation (Garcia et al., 2008; Merath, 2008),

$$\cos\theta_1 = \frac{I}{\gamma_{LG}}\Delta\rho - 1 = \frac{I}{\gamma_{LG}}(\rho_{lf} - \rho_g) - 1 \tag{8}$$

where I is the van der Waals potential integral; ρ_g is the bulk density of the gas and ρ_{lf} is the density of the liquid-like film of vapor and equates to the density of the bulk liquid in a one component system (See Text S4 of Supporting Information S1 for more information). Substituting Equation 8 into Equation 6 gives,

$$\cos\theta^* = f_1\frac{I}{\gamma_{LG}}(\rho_{lf} - \rho_g) - 1 \tag{9}$$

A specific substrate and fluid composition at a constant temperature, $\frac{I}{\gamma_{LG}}$ remains constant with pressure (Al-Yaseri et al., 2016). According to Equation 9, any change in contact angle with pressure, for a specific fluid, is controlled by changes in CO_2-density and f_1, alone. Therefore, when the contact angle in the air is measured and therefore defined, the contact angle at any other pressure CO_2 can be calculated. This model is used to obtain the pressure-dependent wettability alteration of a given gas-solid-water system under constant temperature. There are three assumptions in this model: (a) water and CO_2 are two immiscible phases, and the potential formation of H_2CO_3 is neglected; (b) the surface of the coal pores is considered an ideal smooth surface, regardless of roughness; (c) the coal is 100% water-saturated and the water replaced by CO_2 is assumed completely drained from the pores in our NMR experiments.

In this study, we measured the contact angle of distilled water on three coal samples in air at atmospheric pressure, as shown in Table 1. We then obtain contact angles in CO_2 and at different pressures from Equation 9 (Figure 8d). In Equation 9, the values of ρ_g with different pressure at 25°C are obtained from the NIST REFPROP database (NIST, 2021). Since the change in water density with pressure is negligible, the value of ρ_{lf} is set as 1,000 kg/m^3, throughout. The ratio of the solid-liquid interface to the total area, f_1, is obtained from the T_2 spectra under CO_2

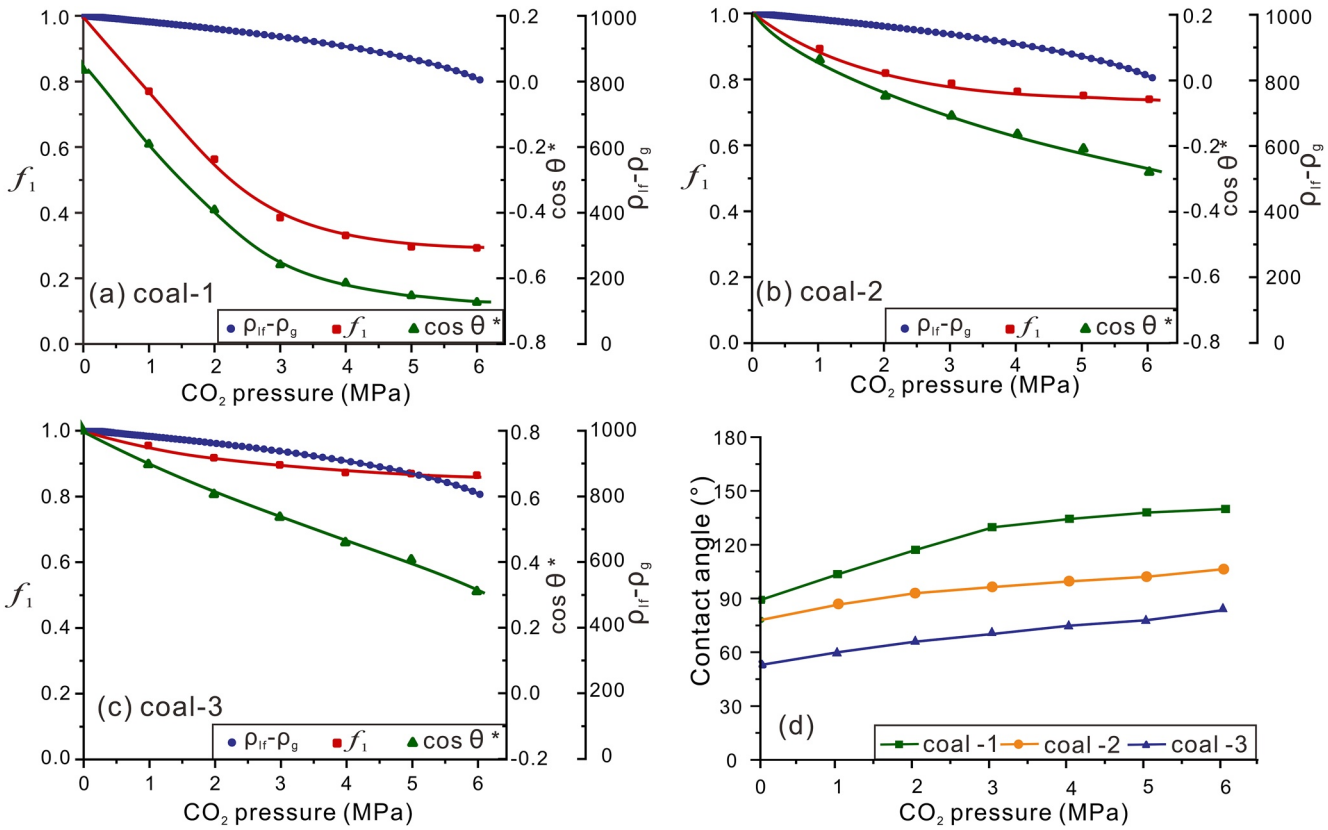

Figure 8. (a–c) Changes in f_1, $(\rho_{lf} - \rho_g)$ and $\cos\theta^*$ with CO_2 pressure (the data is provided Table S1 in Supporting Information S1); (d) contact angle for different CO_2 pressures applied to coal samples.

pressure (see Section 3.4). As shown in Figure 8a–8c ($\rho_{lf} - \rho_g$), f_1 and $\cos\theta^*$ decrease with increasing pressure. Here, the derivatives of ($\rho_{lf} - \rho_g$), f_1 and $\cos\theta^*$ with respect to pressure are also calculated, with these representing trends in change within the data, as shown in Figure 9. As described by the Langmuir isotherm model, the adsorption capacity increases with an increase in gas pressure and asymptotes to a maximum adsorption capacity (Langmuir, 1918). Therefore, f_1 decreases with increasing CO_2 pressure and asymptotes to a constant when CO_2 adsorption reaches saturation, as shown in Figure 8. For bituminous coal-2 and coal-3, when pressure is low (<~4 MPa), then observed changes in contact angle are contributed by CO_2 adsorption A and the increase in CO_2 density. However, when pressure is greater than 4 MPa, f_1 asymptotes to a constant as $\cos\theta^*$ and ($\rho_{lf} - \rho_g$)

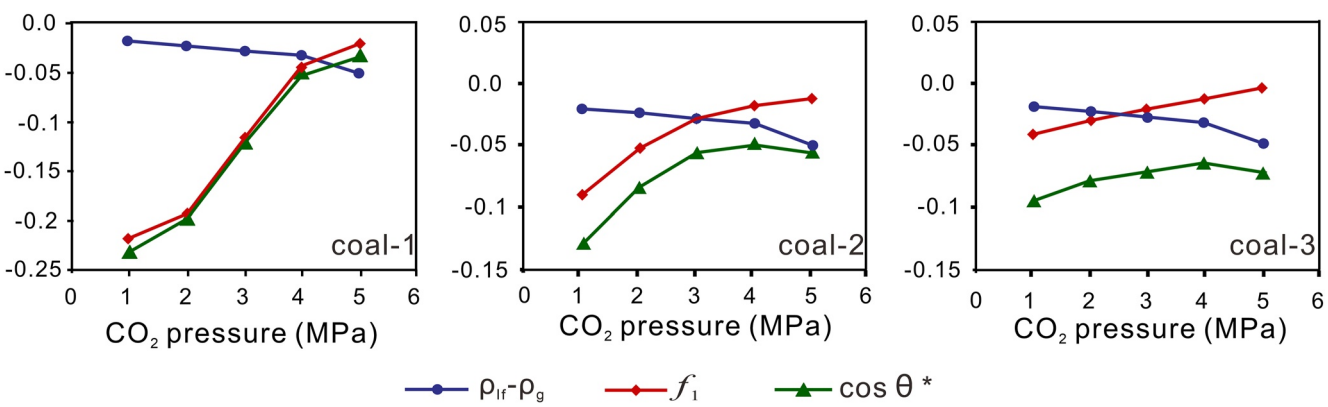

Figure 9. Derivative of f_1, $(\rho_{lf} - \rho_g)$ and $\cos\theta^*$ with CO_2 pressure for different coal samples.3.5 Influence of temperature on coal wettability.

continuously decrease. In this case, the decrease in cos θ^* results mainly from changes in density. However, for the anthracite (coal-1) the changes in f_1 are significant, and the changes in density are relatively weak. Specifically, as shown in Figure 9, the derivatives of cos θ^* and f_1 are very close for coal-1, indicating that the trends in change of cos θ^* is highly consistent with that for f_1. That is, the changes in contact angle are mainly contributed by CO_2 adsorption. Since high-rank coals have a high adsorption capacity for CO_2 (Garnier et al., 2011), CO_2 adsorption plays a decisive role in wettability alteration for the anthracite coal-1 within this experimental pressure range. However, as shown in Figure 8, the f_1 of coal-1 also asymptotes to a constant and the effect of $(\rho_{lf} - \rho_g)$ will be stronger than f_1 at some pressure greater than 6 MPa. This model explains the similar increase in the contact angle to that of the gas sorption isotherm for low to high rank coals, as noted by Arif et al. (2016a).

3.6. Influence of Temperature on Coal Wettability

In addition to pressure, temperature is another important factor that influences coal wettability. This is clear from Equation 6 where both f_1 and contact angle between water and a pure substrate (θ_1) are influenced by temperature.

Since adsorption is an exothermic process, the sorption capacity of coals tends to decrease with increasing temperature (Sakurovs et al., 2008). Thus, increasing temperature increases f_1. When only the effect of gas adsorption is considered, the contact angle decreases with increasing temperature. On the other hand, the effect of temperature on the contact angle between water and pure substrate (θ_1) is complex (Arif et al., 2019). The majority of prior experimental studies agree that contact angle increases with an increase in temperature (Al-Yaseri et al., 2016; Sarmadivaleh et al., 2015). However, some other studies show the converse that contact angles decrease with temperature (Arif, Al-Yaseri, et al., 2016; Saraji et al., 2014). As a consequence, the detailed functional and mechanistic influence of temperature on coal wettability remains open and undefined.

4. Implications for the CO_2 Geo-Sequestration

This study of CO_2-water interactions and the prediction of CO_2-water-coal wetting behavior bears importance on CO_2 adsorption and multiphase fluid transport in coal seams. This has important consequences in evaluating and maximizing CO_2 storage and/or CH_4 recovery from coalbeds.

The simulations of CO_2 displacing water assist in evaluating the CO_2 adsorption capacity of water-bearing coal beds. When CO_2 is sequestrated into coal beds, it adsorbs to the coal surface and displaces the adsorbed water, while water adsorbed to oxygen functional groups are not displaced. Therefore, in water-bearing coal, water adsorbs to oxygen functional groups and occupies the adsorption sites, thus decreasing CO_2 adsorption (Day et al., 2008; L. Huang et al., 2018). The displaced water has no effect on CO_2 adsorption capacity. The results of the simulations infer that the CO_2 sorption capacity of the coal is reduced up to some critical moisture content, beyond which moisture has no effect on sorption capacity (Day et al., 2008). In addition, there are, of course, other minerals such as clay, that may also affect water and CO_2 adsorption capacity (Loring et al., 2013; Zhu et al., 2020).

Meanwhile, CO_2-water-coal wettability directly impacts capillary pressure (Plug et al., 2008). Capillary pressure (P_c) is the pressure difference across the curved interface between two immiscible fluids and is consistent with the pressure difference along a small capillary tube representative of a porous medium (Fanchi, 2002). The pressure difference is expressed in terms of wetting phase pressures (P_w) and nonwetting phase pressures (P_{nw}), thus: $P_c = P_{nw} - P_w$. It is related to gas-liquid interfacial tension, contact angle, and pore radius by: $P_c = \frac{2\gamma LG\cos\theta}{r}$, where r is the radius of a single cylindrical capillary, moreover, for complex and realistic pore structures in coal, other characteristics of pores, such as pore size distribution, shape, and tortuosity also impact behavior (Liu et al., 2016). For a hydrophilic (water-wet) coal, the directionality of action of the net capillary body force, due to the capillary pressure, opposes CO_2 entry into the pores, which reduces the ability of the gas to enter the coal pores. CO_2 adsorption and the concomitant increase in density weakens the water-wetting propensity of coal, decreases capillary pressure, and elevates CO_2 injectivity. With an increase in coal seam depth, elevated reservoir pressures favor CO_2 wettability and therefore increase CO_2 capacity for sequestration. The prediction of wettability remains equivocal as reservoir temperature is increased (Iglauer, 2017). It is also important to note that the coal swelling increases with increasing pressure and potentially induces significant reductions in permeability

and therefore limits CO_2 flow in coal seams (Pini et al., 2009). As a consequence, it is a complex problem to optimize CO_2 storage conditions that requires consideration of the competing influences of component-dependent wettability and related gas adsorption and impacts on matrix swelling and multiphase permeability.

CO_2-water-coal wettability also exerts a crucial influence on other reservoir properties related to permeability, such as the agglomeration of coal fines. In the process of methane extraction and CO_2 injection, the generation and migration of coal fines may cause a significant reduction in permeability as the coal fines are more hydrophobic and are more likely to agglomerate (Awan et al., 2022). Thus, the increase in coal hydrophobicity in CO_2 aids in the agglomeration of coal fines. In this perspective of coal fines generation, agglomeration potentially fixes coal fines at their source of generation and is helpful in preventing the generation of coal fines. However, in terms of the migration of coal fines, it is disadvantageous, once clusters of coal fines are released, and therefore block flow pathways and reduce the gas/water permeability of coal (Zou et al., 2014).

Additionally, experimental observations identify that methane adsorption into coal is lower than that for CO_2 (Day et al., 2008). Thus, it is assumed that CO_2 has a stronger displacement capacity to water than methane. During CO_2 -ECBM recovery, CO_2 adsorbs to the "dry" coal bed and aids in the desorption of methane and removal of blockage of diffusion/flow pathways (Z. Pan et al., 2010). Therefore, it is suggested that CO_2 enhances methane recovery by both improving desorptions and increasing diffusion/flow capacity. This implication will be discussed in future work.

The foregoing understanding of how CO_2 adsorption affects CO_2-H_2O-coal wetting behavior and accurate prediction of in-situ wettability is also germane in constraining projections of storage capacity and containment security in shale formations.

5. Conclusions

Experimental observations confirm that CO_2 adsorption exerts a significant effect on coal-water-CO_2 wetting behavior. We use, NMR experiments and MD simulations of CO_2-water interaction on coal surface in tandem to decipher how CO_2 adsorption impacts surface composition-, pressure- and temperature-dependent coal wettability.

The MD simulations identify that CO_2 preferentially adsorbs to the coal surface and gathers water molecules to the oxygen functional groups. Meanwhile, a fraction of the water escapes from the substrate, leaving water molecules directly bonded to the remaining oxygen-containing functional groups. CO_2 adsorption alters coal wettability by converting some water-occupied sites on the coal surface into CO_2-occupied sites, transforming the coal surface into a mixed surface comprised of solid and CO_2 gas pockets.

The average contact angle of the heterogeneous coal surface may be characterized by a representative contact angle $\cos\theta^* = f_1(1 + \cos\theta_1) - 1$, where the area of the solid-liquid interface (f_1) shows a linear correlation with CO_2 adsorption capacity, that is, the more CO_2 adsorbs to the coal surface, the less the fractional area f_1. This mechanism confirms the observed experimental dependency of coal wettability with CO_2 adsorption capacity.

Furthermore, on this basis, we provide a rationale to link the change in in situ wettability with CO_2 pressure by linking it directly to CO_2 adsorption and changes in CO_2 density. At constant temperature, the water wettability of coal decreases with an increase in pressure. Under low CO_2 pressure, changes in wettability are contributed directly by CO_2 adsorption and CO_2 density - when CO_2 adsorption reaches saturation at high gas pressure, then changes in wettability are determined primarily by changes in CO_2 density.

Overall, for successful implementation of GCS, illuminations about coal wettability changes in the presence of CO_2 provide a comprehensive understanding of fundamental petrophysical properties in CO_2 geo-storage and further provide guidance for practical issues related to storage capacities and E-CBM recovery.

Data Availability Statement

All MD model parameters are listed in Section 2.3 of the text. Data and Supporting Information for the figures are available online (https://doi.org/10.6084/m9.figshare.17087192.v1).

Acknowledgments
We acknowledge financial support from the National Natural Science Foundation of China (42125205; 41872123; 41830427). We thank the Editor, Associate Editor, and two anonymous reviewers for unusually detailed reviews that greatly added to the clarity and message of the study.

References

Ahmed, T. (2010). *Fundamentals of rock properties, Working guide to reservoir rock properties and fluid flow*. Gulf Professional Publishing.

Al-Yaseri, A. Z., Roshan, H., Lebedev, M., Barifcani, A., & Iglauer, S. (2016). Dependence of quartz wettability on fluid density. *Geophysical Research Letters*, *43*(8), 3771–3776. https://doi.org/10.1002/2016gl068278

Al-Yaseri, A. Z., Roshan, H., Xu, X., Zhang, Y., Sarmadivaleh, M.,Lebedev, M., et al. (2017). Coal wettability after CO_2 injection. *Energy & Fuels*, *31*(11), 12376–12382. https://doi.org/10.1021/acs.energyfuels.7b01189

Arif, M., Abu-Khamsin, S., & Iglauer, S. (2019). Wettability of rock/CO_2/brine and rock/oil/CO_2-enriched-brine systems: Critical parametric analysis and future outlook. *Advances in Colloid and Interface Science*, *268*, 91–113.

Arif, M., Al-Yaseri, A. Z., Barifcani, A., Lebedev, M., & Iglauer, S. (2016). Impact of pressure and temperature on CO_2-brine-mica contact angles and CO_2-brine interfacial tension: Implications for carbon geo-sequestration. *Journal of Colloid and Interface Science*, *462*, 208–215. https://doi.org/10.1016/j.jcis.2015.09.076

Arif, M., Barifcani, A., Lebedev, M., & Iglauer, S. (2016a). CO_2-wettability of low to high rank coal seams: Implications for carbon geo-sequestration and enhanced methane recovery. *Fuel*, *181*, 680–689. https://doi.org/10.1016/j.fuel.2016.05.053

Arif, M., Barifcani, A., Lebedev, M., & Iglauer, S. (2016b). CO_2 wettability of shales and coals as a function of pressure, temperature and rank: Implications for CO_2 sequestration and enhanced methane recovery, Paper presented at PAPG/SPE Pakistan Section *Annual Technical Conference and exhibition*.

Awan, F. U. R., Arif, M., Iglauer, S., & Keshavarz, A. (2022). Coal fines migration: A holistic review of influencing factors. *Advances in Colloid and Interface Science*, *301*, 102595.

Bormashenko, E. (2008). Why does the Cassie-Baxter equation apply? *Colloids and Surfaces A: Physicochemical and Engineering Aspects*, *324*(1–3), 47–50.

Bormashenko, E. (2009). Young, Boruvka-Neumann, Wenzel and Cassie-Baxter equations as the transversality conditions for the variational problem of wetting. *Colloids and Surfaces A: Physicochemical and Engineering Aspects*, *345*(1), 163–165.

Cassie, A., & Baxter, S. (1944). Wettability of porous surfaces. *Transactions of the Faraday Society*, *40*, 546–551.

Chang, S. C., Chien, S. Y., Chen, C. L., & Chen, C. K. (2015). Analyzing adsorption characteristics of CO_2, N_2 and H_2O in MCM-41 silica by molecular simulation. *Applied Surface Science*, *331*, 225–233.

Coates, G. R., Xiao, L. Z., & Prammer, M. G. (1999). *NMR logging principles and applications*: Gulf Publishing Company.

Daryasafar, A., Keykhosravi, A., & Shahbazi, K. (2019). Modeling CO_2 wettability behavior at the interface of brine/CO_2/mineral: Application to CO_2 geo-sequestration-sciencedirect. *Journal of Cleaner Production*, *239*, 118101.

Day, S., Sakurovs, R., & Weir, S. (2008). Supercritical gas sorption on moist coals. *International Journal of Coal Geology*, *74*, 203–214.

Fanchi, J. R. (2002). *Shared Earth earth modeling*. Elsevier Butterworth-Heinemann.

Folger, P. (2018). *Carbon capture and sequestration (CCS) in the United States*. Congressional *Research Service Reports, UNT Digital Library*.

Garcia, R., Osborne, K., & Subashi, E. (2008). Validity of the "Sharp-kink approximation" for water and other fluids. *Journal of Physical Chemistry B*, *112*, 8114–8119.

Garnier, C., Finqueneisel, G., Zimny, T., Pokryszka, Z., Lafortune, S., Défossez, P. D. C., & Gaucher, E. C. (2011). Selection of coals of different maturities for CO_2 storage by modelling of CH_4 and CO_2 adsorption isotherms. *International Journal of Coal Geology*, *87*(2), 80–86.

Godec, M., Koperna, G., & Gale, J. (2014). CO_2-ECBM: A review of its status and global potential. *Energy Procedia*, *63*, 5858–5869.

Gray, I. (1987). Reservoir engineering in coal seams: Part 1-the physical process of gas storage and movement in coal seams. *SPE Reservoir Engineer*, *2*, 28–34.

Gubelin, G., & Boyd, A. (1997). Total porosity and bound-fluid measurements from an NMR tool. *Journal of Petroleum Technology*, *49*(07), 718.

Guo, R., & Kantzas, A. (2009). Assessing the water uptake of Alberta coal and the impact of CO_2 injection with Low-Field NMR. *Journal of Canadian Petroleum Technology*, *48*(7), 40–46.

Gutierrez-Rodriguez, J. A., Purcell, R. J., & Aplan, F. F. (1984). Estimating the hydrophobicity of coal Colloid. *Surfaces*, *12*, 1–25.

Harris, J. G., & Yung, K. H. (1995). Carbon dioxide's liquid-vapor coexistence curve and critical properties as predicted by a simple molecular model. *Journal of Physical Chemistry*, *99*(31), 12021–12024.

Howard, J. J., Kenyon, W. E., & Straley, C. (1993). Proton-magnetic resonance and pore-size variations in reservoir sandstones. *SPE Formation Evaluation*, *8*(03), 194–200.

Huang, L., Ning, Z., Wang, Q., Zhang, W., Cheng, Z., Wu, X., & Qin, H. (2018). Effect of organic type and moisture on CO_2/CH_4 competitive adsorption in kerogen with implications for CO_2 sequestration and enhanced CH_4 recovery - Sciencedirect. *Applied Energy*, *210*, 28–43.

Huang, P. H., & Chen, S. H. (2016). Effect of moisture content, system pressure, and temperature on the adsorption of carbon dioxide in carbon nanotube and graphite composite structures using molecular dynamics simulations. *Journal of Nanoscience and Nanotechnology*, *16*, 8654–8661.

Ibrahim, A. F., & Nasr-El-Din, H. (2019). *Investigation of coal wettability for the CO_2 sequestration and ECBM applications: A review*. Paper presented at Carbon Management Technology Conference.

Iglauer, S. (2017). CO_2-water-rock wettability: Variability, influencing factors, and implications for CO_2 geostorage. *Accounts of Chemical Research*, *50*(5), 1134.

Iglauer, S., Mathew, M. S., & Bresme, F. (2012). Molecular dynamics computations of brine-CO_2 interfacial tensions and brine-CO_2-quartz contact angles and their effects on structural and residual trapping mechanisms in carbon geo-sequestration. *Journal of Colloid and Interface Science*, *386*, 405–414.

IPCC. (2005). *Carbon dioxide capture and storage*. In *Prepared by Working Group III of the IPCC*. Cambridge University Press

Kleinberg, R., Kenyon, W., & Mitra, P. (1994). Mechanism of NMR relaxation of fluids in rock. *Journal of Magnetic Resonance*, *108*, 206–214.

Krainer, S., & Ulrich, H. (2021). Contact angle measurement on porous substrates: Effect of liquid absorption and drop size. *Colloids and Surfaces A: Physicochemical and Engineering Aspects*, *619*, 126503.

Langmuir, I. (1918). The adsorption of gases on plane surfaces of glass, mica and platinum. *Journal of the American Chemical Society*, *40*(9), 1361–1403.

Liu, P., Yuan, Z., & Li, K. (2016). An improved capillary pressure model using fractal geometry for coal rock. *Journal of Petroleum Science and Engineering*, *145*, 473–481.

Loring, J. S., Schaef, H. T., Thompson, C. J., Turcu, R. V., Miller, Q. R., Chen, J., et al. (2013). Clay hydration/dehydration in dry to water-saturated supercritical CO_2: Implications for caprock integrity. *Energy Procedia*, *37*(1), 5443–5448.

Merath, C. (2008). *Microscopic calculation of line tensions. PhD thesis*. University of Stuttgart.

Mosleh, M. H., Sedighi, M., Babaei, M., & Turner, M. (2019). *Geological sequestration of carbon dioxide. Managing global Warming*. Academic Press.

Mukherjee, M., & Misra, S. (2018). A review of experimental research on enhanced coal bed methane (ECBM) recovery via CO_2 sequestration. *Earth-Science Reviews*, *179*, 392–410.
Muster, T. H., & Prestidge, C. A. (2002). Application of time-dependent sessile drop contact angles on compacts to characterize the surface energetics of sulfathiazole crystals. *International Journal of Pharmaceutics*, *234*(1–2), 43–54.
Nie, B., Liu, X., Yang, L., Meng, J., & Li, X. (2015). Pore structure characterization of different rank coals using gas adsorption and scanning electron microscopy. *Fuel*, *158*(15), 908–917.
NIST. (2021). *REFPROP database*. Retrieved from https://www.nist.gov/programs-projects/reference-fluid-thermodynamic-and-transport-properties-database-refprop
NOAA. (2021). *Carbon dioxide peaks near 420 parts per million at Mauna Loa observatory*. Retrieved from https://research.noaa.gov/article/ArtMID/587/ArticleID/2764/Coronavirus-response-barely-slows-rising-carbon-dioxide
Pan, J., Zhu, H., Hou, Q., Wang, H., & Wang, S. (2015). Macromolecular and pore structures of Chinese tectonically deformed coal studied by atomic force microscopy. *Fuel*, *139*(1), 94–101.
Pan, Z., Connell, L. D., Camilleri, M., & Connelly, L. (2010). Effects of matrix moisture on gas diffusion and flow in coal. *Fuel*, *89*, 3207–3217.
Pini, R., Ottiger, S., Burlini, L., Storti, G., & Mazzotti, M. (2009). Role of adsorption and swelling on the dynamics of gas injection in coal. *Journal of Geophysical Research: Solid Earth*, *114*, B04203. https://doi.org/10.1029/2008JB005961
Plug, W., Mazumder, S., & Bruining, J. (2008). Capillary pressure and wettability behavior of CO_2 sequestration in coal at elevated pressures. *SPE Journal*, *13*(04), 455–464.
Price, W. S., Ide, H., & Arata, Y. (1999). Self-diffusion of supercooled water to 238 K using PGSE NMR diffusion measurements. *Journal of Physical Chemistry A*, *103*(4), 448–450.
Sakurovs, R., Day, S., Weir, S., & Duffy, G. (2008). Temperature dependence of sorption of gases by coals and charcoals. *International Journal of Coal Geology*, *73*(3–4), 250–258.
Sakurovs, R., & Lavrencic, S. (2011). Contact angles in CO_2-water-coal systems at elevated pressures. *International Journal of Coal Geology*, *87*, 26–32.
Saraji, S., Piri, M., & Goual, L. (2014). The effects of SO_2 contamination, brine salinity, pressure, and temperature on dynamic contact angles and interfacial tension of supercritical CO_2/brine/quartz systems. *International Journal of Greenhouse Gas Control*, *28*, 147–155.
Sarmadivaleh, M., Al-Yaseri, A. Z., & Iglauer, S. (2015). Influence of temperature and pressure on quartz-water-CO_2 contact angle and CO_2-water interfacial tension. *Journal of Colloid and Interface Science*, *441*, 59–64.
Schön, J. H. (2011). *Handbook of Petroleum Exploration and production*. Elsevier. Physical *properties of rocks*.
Shojai Kaveh, N., Wolf, K. H., Ashrafizadeh, S. N., & Rudolpha, E. S. J. (2012). Effect of coal petrology and pressure on wetting properties of wet coal for CO_2 and flue gas storage. *International Journal of Greenhouse Gas Control*, *11*, S91–S101.
Straley, C., Rossini, D., Vinegar, H., Tutunjian, P., & Morriss, C. (1997). Core analysis by low-field NMR. *Log Analyst*, *38*, 84–93.
Sun, X., Yao, Y., Liu, D., Elsworth, D., & Pan, Z. (2016). Interactions and exchange of CO_2 and H_2O in coals: An investigation by low-field NMR relaxation. *Scientific Reports*, *6*, 19919.
Thakur, P. (2019). *Advanced mine ventilation*. Woodhead Publishing.
White, C., Smith, D. H., Jones, K. L., Goodman, A. L., Jikich, S. A., Lacount, R. B., et al. (2005). Sequestration of carbon dioxide in coal with enhanced coalbed methane recovery-a review. *Energy & Fuels*, *19*(3), 659–724.
Wu, Y., Tepper, H. L., & Voth, G. A. (2006). Flexible simple point-charge water model with improved liquid-state properties. *The Journal of Chemical Physics*, *124*, 024503.
Yao, Y., Liu, D., Che, Y., Tang, S., & Huang, W. (2010). Petrophysical characterization of coals by low-field nuclear magnetic resonance (NMR). *Fuel*, *89*, 1371–1380.
Yao, Y., Liu, D., Liu, J., & Xie, S. (2015). Assessing the water migration and permeability of large intact bituminous and anthracite coals using NMR relaxation spectrometry. *Transport in Porous Media*, *107*(2), 527–542.
You, X. F., Wei, H. B., Zhu, X. C., Lyu, X. J., & Li, L. (2018). Role of oxygen functional groups for structure and dynamics of interfacial water on low rank coal surface: A molecular dynamics simulation. *Molecular Physics*, *116*, 1670–1676.
Zhu, H., Ju, Y., Huang, C., Chen, F., & Yu, K. (2020). Microcosmic gas adsorption mechanism on clay-organic nanocomposites in a marine shale. *Energy*, *197*, 117256.
Zou, Y. S., Zhang, S. C., & Zhang, J. (2014). Experimental method to simulate coal Fines migration and coal Fines aggregation prevention in the hydraulic fracture. *Transport in Porous Media*, *101*(1), 17–34.

References From the Supporting Information

Meiboom, S., & Gill, D. (1958). Modified spin-echo method for measuring nuclear relaxation times. *Review of Scientific Instruments*, *29*(8), 688–691.
Meunier, M. (2012). Introduction to materials Studio. *Presented at The European Physical Journal Conferences*, *30*, 04001.
Roshan, H., Al-Yaseri, A. Z., Sarmadivaleh, M., & Iglauer, S. (2016). On wettability of shale rocks. *Journal of Colloid and Interface Science*, *475*, 104–111.
Telkki, V. V., Urbańczyk, M., & Zhivonitko, V. (2021). Ultrafast methods for relaxation and diffusion. *Progress in Nuclear Magnetic Resonance Spectroscopy*, *126–127*, 101–120.